Drug Design, Development and Therapy

Dovepress
Taylor & Francis Group

Open Access Full Text Article

ORIGINAL RESEARCH

Anemarrhena asphodeloides Bunge-*Fritillaria Cirrhosae* Bulbus Herb Pair Alleviates Ovalbumin-Induced Asthma by Regulating Arachidonic Acid Pathway

Xi Tian[1,2,*], Qingfei Cui[3,*], Jinhuan Wei[1], Qian Zhang[1], Huiyi Zhang[1], Mengxin Yang[1], Yiqi Xing[4], Yukun Niu[1], Wenyu Li[1], Nan Wang[1], Yiran Jin[5], Yingfeng Du[1]

[1]Department of Pharmaceutical Analysis, School of Pharmacy, Hebei Medical University, Shijiazhuang, Hebei, People's Republic of China; [2]Institute of Cash Crop, Hebei Academy of Agriculture and Forestry Sciences, Shijiazhuang, Hebei, People's Republic of China; [3]Shijiazhuang Biomedical Academician Workstation, Shijiazhuang Yiling Pharmaceutical Co., Ltd., Shijiazhuang, Hebei, People's Republic of China; [4]Architectural Engineering Institute, Hebei Vocational University of Industry and Technology, Shijiazhuang, Hebei, People's Republic of China; [5]Department of Pharmacy, The Second Hospital of Hebei Medical University, Shijiazhuang, Hebei, People's Republic of China

*These authors contributed equally to this work

Correspondence: Yingfeng Du, Department of Pharmaceutical Analysis, School of Pharmacy, Hebei Medical University, Shijiazhuang, Hebei, People's Republic of China, Tel +86-311-86265625, Fax +86-311-86266419, Email 17700941@hebmu.edu.cn; Yiran Jin, The Second Hospital of Hebei Medical University, Shijiazhuang, Hebei, People's Republic of China, Email jinyiran@sohu.com

Drug Design, Development and Therapy downloaded from https://www.dovepress.com/
For personal use only.

Background: In traditional Chinese Medicine (TCM), Zhimu (*Anemarrhena asphodeloides* Bunge, ZM) - Chuanbeimu (*Fritillaria Cirrhosae* Bulbus, CBM) (ZC) is one of the most classical herb pairs used in the treatment of lung diseases such as asthma. This study aimed to investigate how ZC affects asthma and its mechanism.

Methods: Asthma model rats were sensitized by ovalbumin. The anti-asthma efficacy of ZM, CBM and ZC were evaluated through analysis of lung function, pathological sections and biochemical indices. Metabolomics based on UHPLC-QTOF-MS was conducted to determine the synergistic anti-asthma effect of combination therapy. Asthma targets and mechanism prediction were performed using network pharmacology. Then, the potential anti-asthma mechanism of ZC was explored using RT-qPCR.

Results: According to the lung function test, Hematoxylin-Eosin Staining experiment, ZC herb pair had an obvious anti-asthma effect over either ZM or CBM alone. It has also been demonstrated that positive effect of ZC against Th1/Th2 immune imbalance. Both metabolomics and network pharmacology were highly enriched in the arachidonic acid metabolism pathway. The mRNA expression levels of ALOX5, PLA2G4A and CYP1A2, critical targets in arachidonic acid metabolism, were significantly down-regulated by RT-qPCR.

Conclusion: By reducing the expression of cytokines and chemokines mediated by the arachidonic acid metabolism pathway, ZC could alleviate OVA-induced asthma in vivo. It was the first to demonstrate the complex mechanism of ZC for the treatment of asthma. Meanwhile, a new paradigm was established for evaluating the pharmacological effects of TCM drugs for asthma based on multiple mechanisms.

Keywords: *Anemarrhena asphodeloides* Bunge-*Fritillaria Cirrhosae* Bulbus, anti-asthma, combination mechanisms, network pharmacology, metabolomics, RT-qPCR

Introduction

Asthma, short for bronchial asthma, is an inflammatory lung disease characterized by reversible obstruction, inflammation, and increased sensitivity to various stimuli.[1,2] According to the 2020 Global Asthma Prevention and Control Initiative, the incidence of asthma exceeded 300 million worldwide, with over 40 million people in China. Due to factors, such as decreased air quality and an increase in obesity, the number of patients is still continuously increasing, and asthma has become an increasing threat to the global public health that urgently needs to be addressed. Current drug treatments for asthma included corticosteroids, beta-agonists, leukotriene antagonists, anticholinergic drugs and

Received: 7 January 2025
Accepted: 20 May 2025
Published: 27 May 2025

© 2025 Tian et al. This work is published and licensed by Dove Medical Press Limited. The full terms of this license are available at https://www.dovepress.com/terms.php and incorporate the Creative Commons Attribution – Non Commercial (unported, v4.0) License (http://creativecommons.org/licenses/by-nc/4.0/). By accessing the work you hereby accept the Terms. Non-commercial uses of the work are permitted without any further permission from Dove Medical Press Limited, provided the work is properly attributed. For permission for commercial use of this work, please see paragraphs 4.2 and 5 of our Terms (https://www.dovepress.com/terms.php).

Graphical Abstract

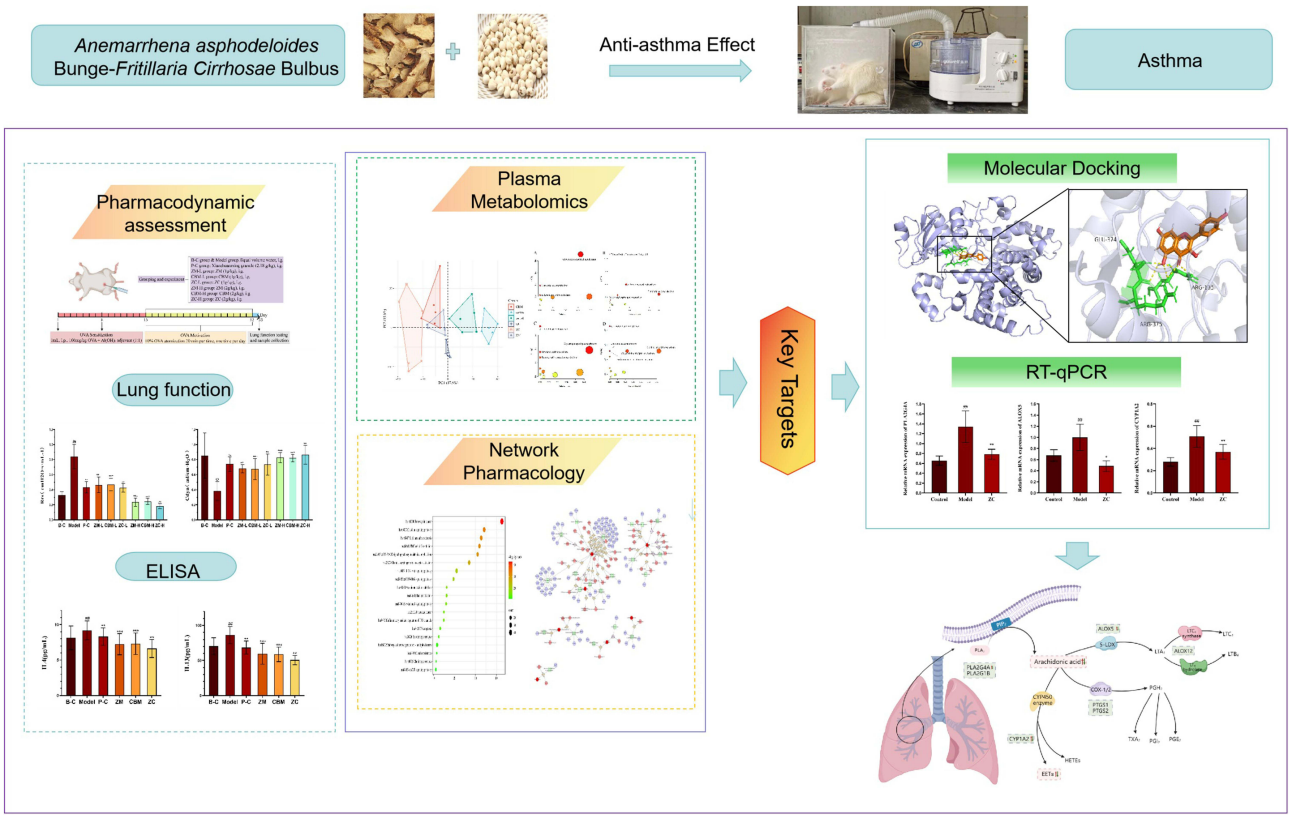

immunotherapy.[3,4] In some cases, therapies currently in clinical use are prone to tolerance and adverse reactions, which cannot simultaneously treat acute attacks and control asthma symptoms.[5,6] Therefore, anti-asthma drugs with multiple targets, high-efficiency, and low toxicity still need to be developed.

There are multiple targets and complex components in Chinese herbal medicine, which allows it to be developed into excellent anti-asthma treatments.[7,8] Zhimu-Chuanbeimu (ZC, *Anemarrhena asphodeloides* Bunge-*Fritillaria Cirrhosae* Bulbus, 1:1) as a famous herb pair has a long history of application, which was first recorded in famous ancient Chinese books such as "Jingyue Quanshu" and "Emergency Immortal Formula". There are many traditional Chinese prescriptions including ZC herb pair such as Ermu San (from "Zhengzhi Yaojue Leifang"), Ermu Ningshuo Wan (from "Zhengyin Maizhi"), Ermu Shigao Tang (from "Gongjin Yijian"), etc.,[9–12] which were widely used to treat phlegm heat cough syndrome. Additionally, pharmacological experiments have shown that both Zhimu (ZM) and Chuanbeimu (CBM) have anti-asthma effects alone, and the combination of ZM and CBM could enhance these effects.[13] According to traditional Chinese medicine theory, ZM is good at clearing lung heat, while CBM is good at resolving phlegm and stopping cough. The combination of the two can achieve both clearing heat and resolving phlegm, making it suitable for asthma with heat phlegm obstructing the lungs.[13] Zhimu saponins had significant pharmacological effects such as anti-inflammatory and antioxidant effects and could significantly inhibit the degranulation of mast cells and release of histamine[14] Chuanbeimu alkaloids could significantly inhibit the cough frequency induced by ammonia water in mice, increase the cough latency period, and significantly increase the output of phenol red in the trachea of mice, producing a significant expectorant effect.[15] The two have component synergy and complementary effects in anti-inflammatory and airway dilation. CBM is a typical traditional Chinese medicine (TCM) with multiple botanical sources including *Fritillaria cirrhosa* D. Don, *Fritillaria unibracteata* Hsiao et K.C. Hsia, *Fritillaria przewalskii* Maxim., *Fritillaria delavayi* Franch., *Fritillaria taipaiensis* P.Y. Li and *Fritillaria unibracteata* Hsiao et K.C. Hsiavar. Wabuensis. Based on previous research on

different sources of CBM and traditional Chinese medicine theory, combined with clinical medication habits in TCM, the use of *Fritillaria cirrhosa* D. Don in the selection of varieties for the treatment of cough and asthma in the ZC drug pair is more effective in accordance with clinical syndrome differentiation.[16,17] Previous studies have shown that ZC compatibility could significantly alter the pharmacokinetic behavior of active ingredients, suggesting the possibility of drug efficacy synergy.[18] Nevertheless, the potential mechanism of synergistic effect of this herb still remains unclear.

Because there are multiple compounds, targets, and pathways, conventional experimental methods have difficulty dissecting synergetic mechanisms. Network pharmacology and metabolomics can provide insights into the potential combination mechanisms of TCM.[19,20] As a well-established histological technique in the post-genomic era, metabolomics has long been utilized in TCM. A major goal of this research is to identify a number of endogenous low-molecular metabolites in response to both internal and external signals and provide clues about the molecular basis and mechanisms of action. In addition, it could contribute to the assessment of disease control rates and elucidating how TCM works.[21] Network pharmacology is an integrated pharmacology-pharmacodynamic approach to constructing and analyzing networks. It involves the application of omics and systems biology technologies in a novel research field.[22,23] The latest developments in network pharmacology have provided a comprehensive understanding of the complex interactions between bioactive components and potential mechanisms of TCM.[24] Combining metabolomics with network pharmacology is more conducive to the enrichment analysis of biological information, as well as the exploration of core targets and pathways. Furthermore, the application of RT-qPCR can prove the reliability of the data. The use of molecular docking in structural molecular biology and computer-aided drug design is of great importance.[25] It was used to describe intermolecular interactions between proteins and ligands for predicting the poses of multiple ligands and discovering novel promising bioactive compounds more accurately.[26]

In this paper, the collaborative anti-asthma effect of ZC herb pair was assessed by the asthma rat model. Then, a plasma metabolomic analysis was performed to reveal the synergetic metabolic mechanisms in terms of metabolites and metabolic pathways. Subsequently, a network pharmacology approach was used to discover the combination of targets, pathways, and mechanisms of ZC for anti-asthma. To elucidate potential connections, a compound-response-enzyme-gene network was constructed. Finally, molecular docking was used to predict the interaction between active components and key targets. The potential anti-asthma mechanism of ZC was validated and explored through RT-qPCR (Figure 1). To our knowledge, this was the first study that has combined network pharmacology and plasma metabolomics to investigate the anti-asthma mechanism of a ZC herb pair.

Materials and Methods

Materials and Reagents

Both acetonitrile (ACN; LC/MS grade) and methanol (MeOH; LC/MS grade) were provided by TEDIA Company (USA). Thermo Fisher Scientific (Shanghai, China) provided UHPLC-grade formic acid. The HPLC grade ethanol was purchased from Tianjin Fuyu Fine Chemical Co. Ltd (Tianjin, China) and was used to prepare herb extracts. Wahaha Group Co. Ltd. (Hangzhou, China) supplied the purified water.

Xiaochuanning granule was purchased from Guizhou Ruicheng Pharmaceutical Co., Ltd. Both *Fritillaria cirrhosa* D. Don and *Anemarrhena asphodeloides* Bge. were purchased from the Anguo Medicinal Materials Market in Baoding, Hebei Province. Professor Yun Huang (Department of Pharmacognosy, School of Pharmacy, Hebei Medical University, Shijiazhuang, PR China) identified and stored all medicinal materials and vouchers (Number: 20201015) in the herbarium of the College of Pharmacy, Hebei Medical University.

Preparation of Herbs Extracts

ZM (90 g), CBM (90 g), and ZC (90 g, 1:1, w/w) were extracted twice with 70% ethanol for 1 hour, respectively. After combining the extraction solutions, ethanol was removed under reduced pressure by filtering. In the next step, extracts were concentrated in a vacuum and then lyophilized into powder and stored at −80°C (the drug-extract ratio was 38.3%, 8.0%, and 41.7% respectively).

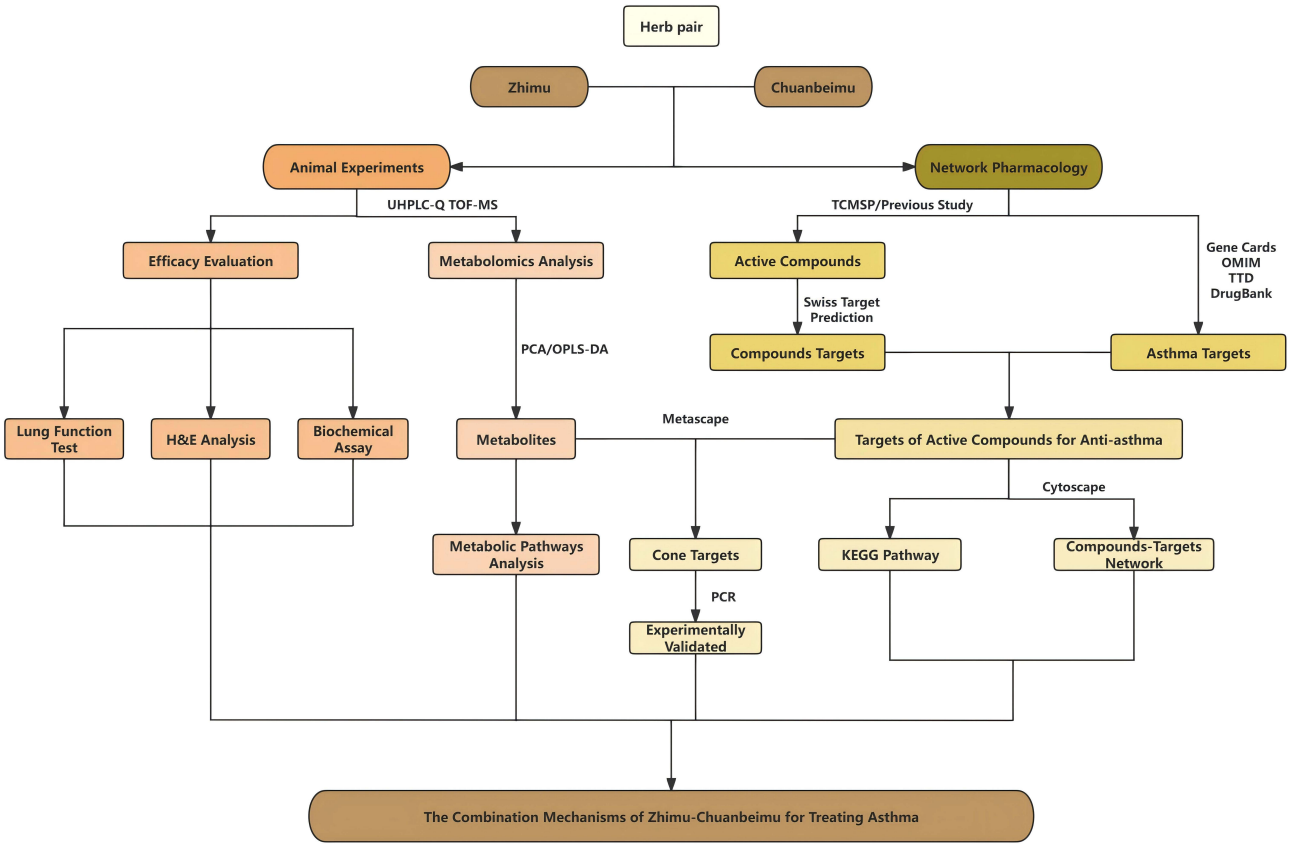

Figure 1 Workflow for dissecting the combination mechanisms of ZC for treating asthma.

UHPLC-QTOF-MS Identifying Compounds of ZC Extract

An UHPLC-QTOF-MS methodology was developed for the comprehensive profiling of ZC components. This was executed using a SHIMADZU LC-30A system (SHIMADZU, Japan), interconnected with an AB SCIEX Triple TOF™ 5600+ system featuring a DuoSpray™ Turbo V Source (AB SCIEX, USA). Chromatographic separations took place on a Phenomenex Kinetex C18 column (2.1 × 100 mm, 1.7 µm, Phenomenex, USA), maintained at a temperature of 30°C. A flow rate of 300 µL/min was sustained, with an injection volume of 5 µL. The mobile phase comprised (A) water containing 0.1% formic acid and (B) acetonitrile. The gradient elution profile for the mobile phase entailed: 0–1 min, 5% B; 1–4 min, 5–20% B; 4–15 min, 20–26% B; 15–21 min, 26–40% B; 21–25 min, 40–95% B; 25–26 min, 95–5% B. Following this, a 5-minute post-run period was allowed for instrument equilibrium before the subsequent injection.

Electrospray ionization (ESI)-generated mass spectrum (MS) data were acquired in both positive and negative ion modes. The acquisition of MS spectra was carried out using Analyst TF 1.7 software (AB SCIEX), leveraging the Information Dependent Acquisition (IDA) function with dynamic background subtraction incorporated. Optimal operational parameters for the MS were established as follows: declustering potential (DP) at 90 V or −90 V, collision energy (CE) at 45 eV or −45 eV, and collision energy spread (CES) at 20 eV for MS/MS. The mass spectrometry scan ranges were configured to *m/z* 100–1200 for MS scans and *m/z* 50–1000 for MS/MS scans. Each MS experiment had an accumulation time of 250 ms, while MS/MS had 80 ms. In the IDA experiments, the eight most intense ions from every full MS scan were chosen for MS/MS fragmentation. The approach for compound identification in ZC was consistent with a method detailed in a prior publication.[27,28]

Construction of Asthma Rats Model

Male Sprague-Dawley rats (180 ± 20 g) were provided by Liaoning Changsheng Biotechnology Co., Ltd (SCXK 2019–0001). All animal studies were conducted according to the Guide for Care and Use of Laboratory Animals approved by the Hebei Medical University Ethics Committee (IACUC-Hebmu-2022134, Approval Date: March 28, 2022).

The experimental procedure of the in vivo asthma rat model is shown in Figure 2A. Fifty-four rats were randomly divided into 9 groups, 6 rats in each group: (1) blank control group (B-C group), (2) model group, (3) positive control group (Xiaochuanning granule, 2.18 g/kg; P-C group); (4) Low dose ZM group (1 g/kg), (5) Low dose CBM group (1 g/kg), (6) Low dose ZC group (1 g/kg), (7) High dose ZM group (2 g/kg), (8) High dose CBM group (2 g/kg), (9) High dose ZC group (2 g/kg). Except for the blank control group, the other eight groups were sensitized by freshly prepared OVA aluminum hydroxide solution (1 mL, i.p. containing 100mg/mL OVA NaCl solution and equal volume $Al(OH)_3$ adjuvant) on day 1 and day 8, respectively. The blank group was injected with the same volume NaCl solution. On day 15 of the experiment, all animals except for the blank control group received 10% OVA aerosol in saline (10 mL) for 30 minutes every day for 17 days in a closed box, via ultrasonic nebulizer connected to the box. Animals of administration groups were orally administered with positive control drug, ZM, CBM, ZC 30 min before the OVA challenge began on day 15 and lasts for 17 days. The entire experiment lasted for 32 days. This experiment set a concentration gradient with clinical equivalent dose as low dose and twice the clinical equivalent dose as high dose.

Rat Lung Function Test

On day 33, after anesthetizing the rats (20% urethane, i.p., 1.2 g/kg, n = 6), pulmonary function tests were performed using the AniRes 2005 lung function meter (Peking Biolab Tech Company, Beijing, China) in accordance with the guidelines provided by the manufacturer. The rats were inserted with an endotracheal tube, which was connected to the ventilator's outlet. Then, the rats were immediately placed supine in a sealed whole-body plethysmograph and connected to a computer-controlled ventilator through the tracheal cannula. Each of the subjects was subjected to mechanical ventilation at a pace of 90 respirations per minute, with an air displacement of 5 milliliters per kilogram of body weight and a breathing cycle ratio of 1.5 to 1.0 during exhalation and inhalation, managed by a computerized small animal ventilator with assistive features. The parameters of lung function, including expiratory resistance (Rrs) and lung dynamic compliance (Cydn), are measured after 30 normal respiratory cycles. A total of five lung function tests were performed on each animal. Data was analyzed using AniRes 2005 software (Beijing Beilangbo Technology Co. Ltd., Beijing, China). The differences between the groups were assessed by *t*-test. Differences with $P < 0.05$ indicated statistical significance.

Sample Collection

After measurement of lung function, blood (n = 6) was collected from the abdominal aorta. The plasma was collected after 4000 rpm centrifugation for 10 min and stored at −80°C until analysis. The lung was taken out, flushed with normal saline. The right lung was immediately fixed with 10% neutral formalin for histological analysis, and the left lung was divided into three parts and immediately frozen in liquid nitrogen for biochemical assay, metabolomics analysis and real-time quantitative PCR, and stored at −80°C. Finally, the rats were euthanized in a sealed container containing 5% isoflurane.

Histological Analysis and Biochemical Assay

After being fixed for 72h, the lung tissue samples (n = 6) were blocked in paraffin after passing through an ascending alcohol series and becoming transparent after passing through an ascending xylene series. Lung tissues samples (5 μm) were sectioned and stained with hematoxylin and eosin (H&E) and then examined under a light microscope.

Each sample of lung tissue was assessed for the type, severity, and extent of lung lesions, as well as the degrees of inflammatory cellular infiltration. The severity of lung lesions consisting of inflammatory cell infiltration around bronchioles, inflammatory cells around blood vessels infiltration, bronchial mucosal inflammatory cell infiltration and bronchial/bronchiolar goblet cell hyperplasia were evaluated and graded by two independent pathologists. Using a light microscope, analysis of entire visual fields and 5-point semiquantitative scale (0 = no change, 1 = minimal change, 2 = mild, 3 = moderate, and 4 = marked) was conducted. In semi-quantitative terms, the scores were graded as follows: no injury = score of 0, minimal injury = score of 1 (+), mild injury = score of 2 (++), moderate injury = score of 3 (+++) and marked injury = score of 4 (++++). The median lesion score of each group of rats was taken as the lesion score of that group.

Using enzyme-linked immunosorbent assay (ELISA) kits, a portion of plasma was tested for the level of interleukin-4 (IL-4) and interleukin-13 (IL-13) according to manufacturer's instructions. All kits were purchased from ABclonal

https://doi.org/10.2147/DDDT.S514891

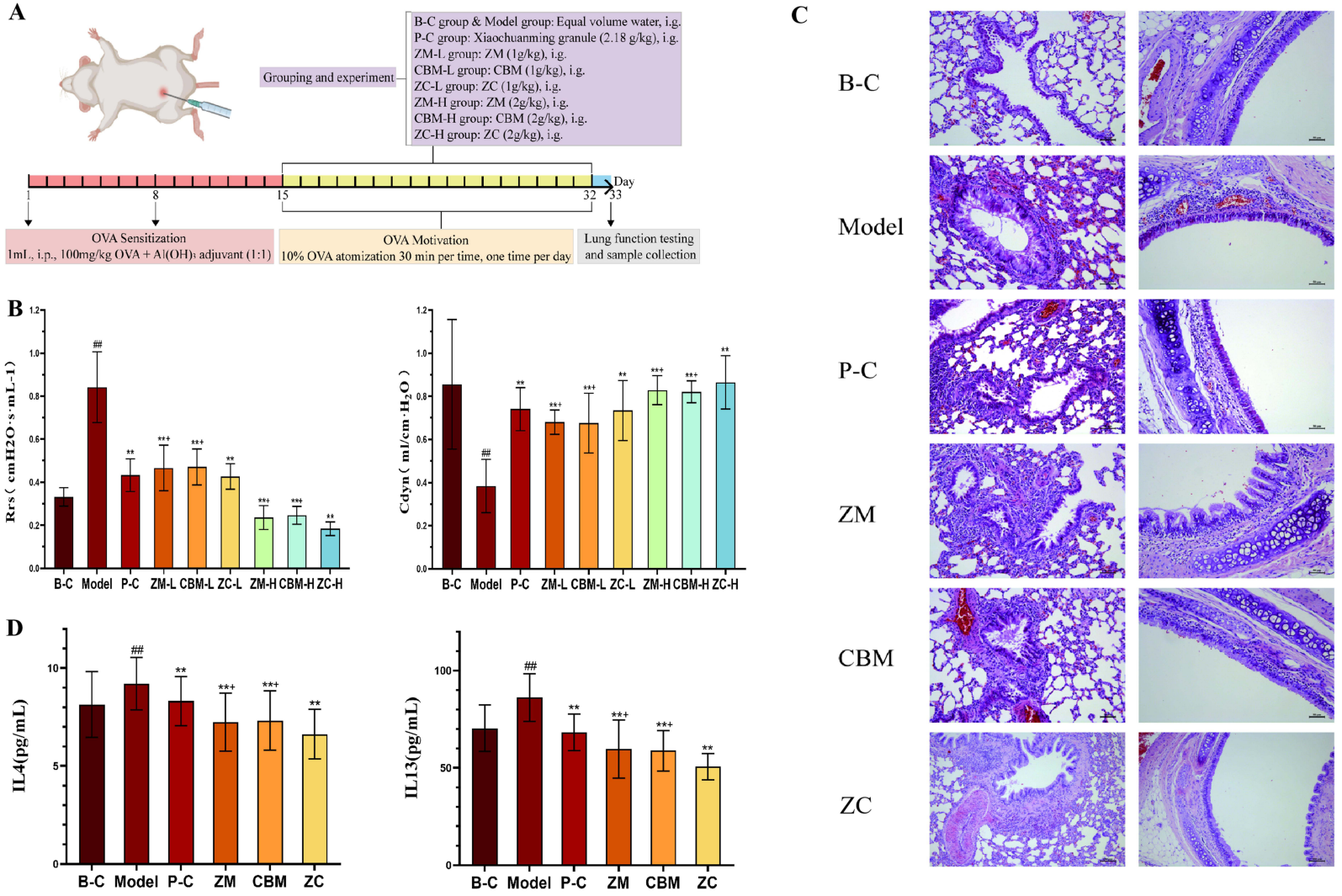

Figure 2 The synergetic anti-asthma effects of ZC (n = 6). (**A**) Establishment of asthma model and drug administration, (**B**) The levels of pulmonary function parameters in each group, (**C**) H&E staining of testis in different groups (200×), (**D**) Plasma levels of IL-4 and IL-13. ($^{\#\#}P < 0.05$ vs Model, $^{**}P < 0.05$ vs Model, $^{+}P < 0.05$ vs ZC.).

Biotech Co., Ltd (USA). A microplate reader (Labsystems Multiskan) was used to measure each well's absorbance at 450 nm. Three independent experiments were performed.

Metabolomics Analysis

After mixing 50 μL plasma samples (n = 6) with 150 μL methanol and vortexing for 5 minutes, the supernatant was centrifuged at 4°C for 10 min at 12000 rpm, and evaporated under a gentle stream of nitrogen to dryness. After drying, the residue was resuspended in 50 μL of acetonitrile-water (50:50, v/v). Following vortexing for 1 min and centrifugation at 12000 rpm for 5 minutes, an aliquot of 5 μL supernatant was injected for metabolomics analysis. A quality control (QC) sample was prepared from each test sample in a volume of 10 μL. In order to ensure that the instrument is stable and performs well, the QC sample was inserted into every five test samples using the same analytical method as the test samples.

Plasma metabolomics data were acquired by a SHIMADZU LC-30A system and an AB SCIEX Triple TOF™ 5600 + system with a DuoSpray™ Turbo V Source (AB SCIEX, Foster City, CA, USA). A chromatographic separation was achieved by a Phenomenex Kinetex C18 (3.0 mm × 100 mm, 2.6 μm). During the experiment, the column temperature was kept at 40°C. Solution A (0.1% formic acid in water) was used as the solvent and solution B (0.1% formic acid in acetonitrile) was used as the mobile phase. It flowed at a rate of 0.3 mL/min. A gradient program of 5% B was followed for 0–2 min, 5–100% B for 2–26 min, and 100% B for 26–30 min. To ensure that the instrument was fully equilibrated after injection, it was allowed to rest for 5 min following injection.

In positive ion mode, ESI was used to collect MS data. Using an IDA function with dynamic background subtraction, MS spectra were acquired by Analyst TF 1.7 software (AB SCIEX). It was determined that the optimal operating conditions for the MS were as follows: ion spray voltage of 5500 V, DP of 60 V, CE of 10 eV for MS, CE of 35 eV and CES of 15 eV for MS/MS. Turbo spray temperature was set to 500°C. Nitrogen was used as both nebulizer and auxiliary gas in this experiment. We set the nebulizer gas (Gas 1), the heater gas (Gas 2), and the curtain gas at 55, 55, and 15 psi, respectively. A mass range of 100–1000 Da was used for TOF MS scans and 50–1000 Da for TOF MS/MS scans. A TOF MS accumulation time of 250 ms was used for the experiments, and a TOF MS/MS accumulation time of 80 ms was used for the experiments. Throughout the run, the calibration delivery system (CDS) with ESI-TOF Calibration Solution (AB SCIEX, United States) was used for mass accuracy maintenance every two hours. Random injections were performed on all real samples.

From the raw LC-MS data, matched peak data was obtained by Progenesis QI 2.2 software (Waters Corporation, Milford, MA). Principal component analysis (PCA) and orthogonal partial least-squares discriminant analysis (OPLS-DA) of the normalized data were conducted using SIMCA-P 14.1 software (Umetrics, Sweden). Stability of the analytical system was assessed through PCA, which was used to identify clustering behavior related to the different data sets in the analysis. Meanwhile, OPLS-DA was used to identify discriminating metabolites that contribute to the classification among the experimental samples. The model's predicative ability and statistical significance were evaluated on the basis of three important model characteristics (R^2X, R^2Y, and Q^2Y) of permutation tests. Based on OPLS-DA, variables relevant for discriminating groups were screened using Variable Importance in Projection (VIP) scores. In addition, significant differences in variables were evaluated using independent t-tests and fold change analysis (FC) in MetaboAnalyst 5.0 software. By using VIPs (VIP > 1), *t*-test ($P < 0.05$) and FC > 1.2 or FC < 0.8, the differential metabolites were selected between the control group and the model group, and between the model group and the administration groups.

The biomarkers were identified according to online databases. There are four databases: KEGG (http://www.kegg.jp), HMDB (http://www.hmdb.ca), METLIN (http://metlin.scripps.edu/) and LIPID MAPS (http://www.lipidmaps.com/). Based on the tentatively identified biomarkers, clustering heatmaps were used to further understand metabolic differences using clustering heatmap by MetaboAnalyst 5.0. We analyzed pathways using MetaboAnalyst 5.0 using parameters ($P < 0.05$) as the index of relevancy.

Component-Target-Pathway-Metabolite Network and Joint Pathway Analysis

A network pharmacology approach was carried out to explore the mechanism of ZC's anti-asthma effects. The compounds' information of ZC was obtained from our previous studies and TCMSP.[16,17] Integrated oral bioavailability (OB) (≥30%) and drug-likeness (DL) (≥0.1)[29] were used to filter the active compounds. Swiss Target Prediction (http://www.swisstargetprediction.ch/) was used to predict the targets of active compounds.[30] Additionally, the database GeneCards,[31] Online

Mendelian Inheritance in Man database (OMIM),[32] TTD,[33] DrugBank[34] were used to collect targets related disease of "asthma". By Venny, the common targets were screened out as the target of ZC in the treatment of asthma. Using the STRING database (version 11.0, https://string-db.org/), we explored protein–protein interactions (PPIs), and targets whose degree was higher than two medians were considered core genes.[35] Cytoscape software version 3.8.2 (National Resource for Network Biology) was used to construct the compound-target network and the PPI network.[36] Using the Metascape online analysis, we performed 15 pathway enrichment analyses (KEGG analysis) based on all proteins/genes.[37] The identified differential metabolites by metabolomics were then imported into the Cytoscape App MetScape. To visualize the interactions between metabolites, pathways, enzymes, and genes, a compound-reaction-enzyme-gene network was constructed.[38] The joint analysis of the targets from network pharmacology and the metabolites from plasma metabolomics were conducted by MetaboAnalyst to select crucial metabolism pathways.[39]

Molecular Docking

The intersection of the two parts above was considered to be the core targets of anti-asthma efficacy by ZC. According to the compound-target network, the components associated with the core targets were selected as the corresponding active compounds. Finally, a molecular docking study was conducted on the key genes and the corresponding active compounds. Data from the PDB database was used to obtain the structural files of protein receptors. MOE software (version 2022.02) was used for subsequent analysis. Genetic algorithms were used to calculate.[40] It is good binding activity with the target protein if the binding energy is less than −5 kcal/mol, which indicates that the ligand can freely bind to the receptor. In addition, PyMOL was used to visualize docking results with minimal binding energy and distance from best mode.

Real-Time Quantitative PCR

A total of 30 mg of lung tissue (n = 6) was used for RNA extraction with Super Total RNA Extraction Kit by Eastep® (Promega, Shanghai, China). RNA was reverse transcribed and followed the instructions into cDNA using GoScript™ Reverse Transcription Mix, Oligo (dT) (Promega, Shanghai, China). As soon as the cDNA has been mixed with ChamQ Universal SYBR qPCR Master Mix (Vazyme Biotech Co., Ltd., Nanjing, China), the assay was performed. As shown in Table 1, the primer sequences were used to calculate the relative mRNA expression using $2^{-\Delta\Delta Ct}$.

Statistical Analyses

Independent *t* tests used for comparing continuous variables between the two groups, and multiple comparisons were carried out using ANOVA, which were examined for normality before analysis. In this study, the chi-square test was assumed to analyze the data for various clinicopathological factors. Differences with $P < 0.05$ were considered significant.

Results

Identification of Components in ZC Extract

Through the correlation analysis with existing literature and database records, 138 compounds were recognized, encompassing triterpenoids, flavonoids, phenolic acids, and saponins, among others, with 11 compounds being definitively authenticated. The base peak chromatogram for ZC is depicted in Figure S1, and the elaborate MS/MS details and intensity metrics are presented in Table S1. The chemical profile comprised 67 constituents derived from CBM, which included 52 alkaloids, 6 nucleosides, 4 organic acids, 3 flavonoids, and 2 sugars, while ZM contributed 71 components, featuring 46 saponins, 9 flavonoids, 7 alkaloids, 4 lignans, 3 phenylpropanoids, 1 anthraquinone, and 1 organic acid.

Rats Symptoms

As a result of sensitization and excitation by OVA, rats in the model and administration groups were presented with the following symptoms: cyanosis, cough, shortness of breath, irregular breathing, significant tremors in limbs, and reduced activity. Contrary to this, rats in the blank control group exhibited no obvious symptoms. It is noteworthy that rats in the

Table 1 Primer Sequences

Primer	Primer Sequences (5' to 3')	
	Forward Primer	Reverse Primer
PLA2G4A	CAGCACATTATAGTGGAACACCA	AGTGTCCAGCATATCGCCAAA
ALOX5	AGCATGAAAGCAAGGCGCATA	GTACGCATCTACGCAGTTCTG
CYP1A2	CTGGGCACTTCGACCCTTAC	TCTCATCGCTACTCTCAGGGA
GAPDH	ACCACAGTCCATGCCATCAC	TCCACCACCCTGTTGCTGTA

administration group had mild symptoms in comparison with the model groups. However, rats in the administration groups did not vary to a great extent. No rats died during this experiment.

Lung Function Tests

The lung function of rats was assessed and analyzed. As shown in Table S2, Rrs increased significantly in the model group compared to the blank control group ($P < 0.05$), while Cydn decreased significantly ($P < 0.05$). This indicated that there were obvious asthma symptoms in the rats of the model group. In comparison with the model group, the lung function parameters significantly improved after administration (Figure 2B). It can be clearly seen from the graph that the anti-asthma effect of the positive control drug was comparable to that of the low-dose ZC group. And the anti-asthma effects of ZC herb pair were more effective than either ZM or CBM alone. Following the findings that ZM, CBM, and ZC had greater anti-asthma effects at high doses (2 g/kg), a high dose of 2 g/kg ZM, CBM, and ZC was used in subsequent studies.

Lung Tissue Histopathology and Biochemical Assay of Th2 Cytokines

Hematoxylin-Eosin staining results of rat lung tissue sections in each group and inflammation scores are shown in Figure 2C and Table S3, respectively. An H&E staining was performed on lung tissue to determine its histological features. Rats in the control group showed normal histological features. In contrast, pathological features associated with asthma were observed in the group induced by OVA. From moderate-to-severe bronchi and bronchiolar damage with perivascular, massive infarctions of inflammatory cells were observed in the prebronchi and peribronchioles of tissue samples from rats induced with OVA. In addition, moderate goblet cell hyperplasia in bronchi and bronchiolar was noted. There was a marked reduction in pulmonary injury with treatment with positive drug, ZM, CBM and ZC. Lung tissues from positive drug, ZM, CBM and ZC group rats showed slight infiltration of inflammatory cells. In these groups, the incidence and severity of peribronchiolar and perivascular inflammatory cell infiltration, bronchial and bronchiolar goblet cell proliferation decreased. After comparison, the improvement effect of the P-C group on lung lesions was not as significant as other treatment groups. It is worth noting that CBM could obviously alleviate the prebronchiolar inflammation, and ZM and ZC could clearly alleviate the prevascular inflammation. The score showed that the anti-inflammatory effect of ZC was more obvious than ZM or CBM alone.

IL-4 and IL-13 are two cytokines generated by T helper (Th) 2 cell, which participate in the pathogenesis of asthma.[41] IL-4 and IL13 were found to be increased in the bronchoalveolar lavage fluid of asthmatic mice in previous studies.[42] As shown in Figure 2D, the expression of IL-4 and IL-13 genes in the plasma of the OVA-induced group rats was significantly higher than that in the control group ($P < 0.05$). Inflammatory processes are mediated by cytokines IL-4 and IL-13. With the help of ELISA kits, quantitative analysis of the two cytokines can be conducted. Their concentrations in plasma were decreased observed in P-C, ZM, CBM and ZC group compared to OVA-induced group ($P < 0.01$), while the decrease degree in ZC group was significantly higher than ZM group and CBM group ($P < 0.01$). In addition, the decrease degree in ZC group was lower than other three treatment groups.

LC-MS Screening of Plasma Differential Metabolites

Typically based peak intensity chromatograms of plasma samples were analyzed in a positive manner. PCA and OPLS-DA were used to analyze metabolic variation using SIMCA-P 14.1 analysis techniques. Using PCA score plots, model and control groups were clearly separated (Figure 3A). In the meantime, the QC group gathered and confirmed that the

instrument had stable behavior. Figure 3A also showed that all experimental groups were separated to the model group in the LC-MS metabolic profiles. However, the metabolic profiles in the ZM, CBM and ZC group were not closer to the control group than the model group, suggesting that drug intervention not only reversed the metabolic disorders caused by the model but also affected other metabolic pathways to achieve the therapeutic effect. OPLS-DA was used later to further uncover differences and identify significant variables between the control group and the model group as well as the model group and all experimental groups. OPLS-DA model validation was carried out using the permutation test (Figure 3B). Based on the R^2X, R^2Y, and Q^2 of the OPLS-DA model shown in Table S4, the OPLS-DA model showed good fitness and prediction capabilities.

We screened for differential metabolites in the control and model groups based on VIP > 1, $P < 0.05$, and FC > 1.2 or FC < 0.8. As a result, a total of 36 differential metabolites were screened out between control group and model group (Table S5). Seventeen differential metabolites were significantly increased in the model group compared to the control group, while 19 differential metabolites were significantly decreased. ZM could regulate 56 metabolites, and CBM could regulate 52 metabolites. A total of 62 metabolites were regulated by ZC herb pair (Table 2 and Figure 3C). Among them, 26 metabolites were shared regulated by ZM and CBM, and 13 metabolites were uniquely regulated by ZC herb pair.

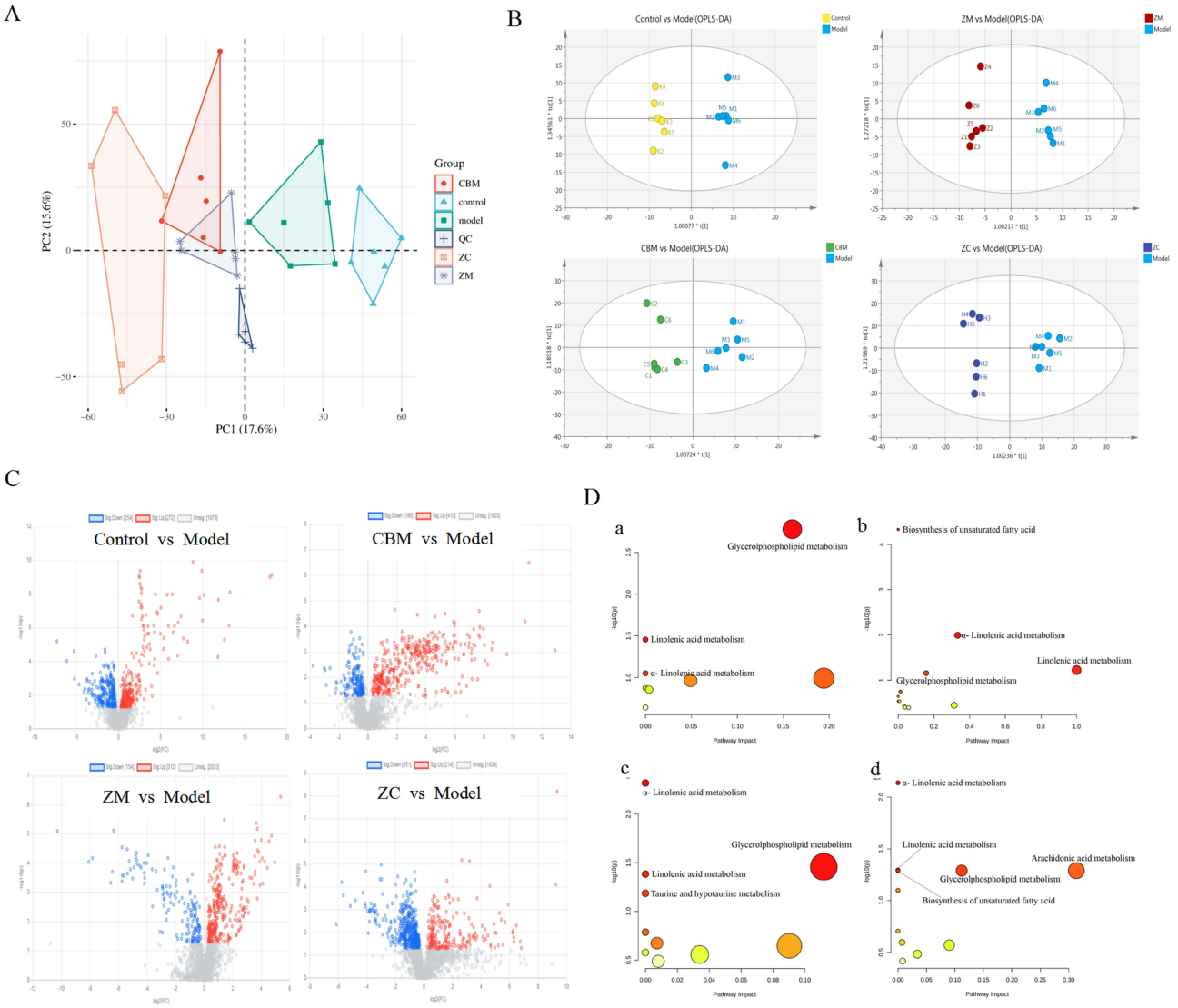

Figure 3 Plasma Metabolomics uncovers the mechanism of ZC for asthma (n = 6). (**A**) PCA score plots, (**B**) OPLS-DA score plots, (**C**) Volcano plots of upregulated and downregulated metabolites, (**D**) Pathway analysis (a: model group; b: ZM group; c: CBM group; d: ZC group).

Table 2 List of Differential Metabolites Between Each Administration Group and Model Group (n = 6)

No	Rt (min)	m/z	Metabolite	Formula	FC[a]	Trend[a]	FC[b]	Trend[b]	FC[c]	Trend[c]
1	0.69	146.16	Spermidine	$C_7H_{19}N_3$	4.1396	Up	2.6281	Up	3.7361	Up
2	1.04	266.05	2'-Deoxycytidine		-	-	0.62967	Down	-	-
3	1.08	235.09	Glu-ser	$C_8H_{14}N_2O_6$	1.2856	Up	-	-	1.479	Up
4	1.10	189.09	N-Acetylglutamine	$C_7H_{12}N_2O_4$	-	-	1.2421	Up	1.412	Up
5	1.17	203.11	L-Acetylcarnitine	$C_9H_{17}NO_4$	0.58195	Down	0.73292	Down	-	-
6	1.17	279.13	N-(1-Deoxy-1-fructosyl) valine	$C_{11}H_{21}NO_7$	0.12861	Down	0.43287	Down	0.33934	Down
7	1.17	160.13	3-Aminooctanoic acid	$C_8H_{17}NO_2$	-	-	-	-	0.34153	Down
8	1.19	294.15	N-(1-Deoxy-1-fructosyl) isoleucine	$C_{12}H_{23}NO_7$	0.059818	Down	0.39712	Down	0.33073	Down
9	1.21	316.14	N-(1-Deoxy-1-fructosyl) leucine	$C_{12}H_{23}NO_7$	0.028114	Down	-	-	0.07256	Down
10	5.75	283.18	Hexaethylene glycol	$C_{12}H_{26}O_7$	-	-	-	-	1.4783	Up
11	6.01	180.07	N-Hydroxytyrosine	$C_9H_{11}NO_4$	-	-	-	-	2.7931	Up
12	6.22	236.13	1,3-Dipropylxanthine	$C_{11}H_{16}N_4O_2$	-	-	-	-	4.6439	Up
13	6.30	326.19	Heptaethylene Glycol	$C_{14}H_{30}O_8$	-	-	-	-	1.5927	Up
14	6.52	218.11	N-Acetylserotonin	$C_{12}H_{14}N_2O_2$	-	-	0.29511	Down	-	-
15	6.74	370.22	Octaethylene glycol	$C_{16}H_{34}O_9$	-	-	-	-	1.6584	Up
16	7.75	520.33	2-Aminoethyl (2R)-2-hydroxy-3-[(2-methoxyoctadecyl) oxy]propyl hydrogen phosphate	$C_{24}H_{52}NO_7P$	1.4615	Up	-	-	1.9836	Up
17	7.94	407.22	Flurogestone Acetate	$C_{23}H_{31}FO_5$	-	-	-	-	7.1292	Up
18	8.19	302.23	Nonanoylcarnitine	$C_{16}H_{31}NO_4$	31.214	Up	-	-	-	-
19	10.64	189.08	Indole-3-propionic acid	$C_{11}H_{11}NO_2$	0.48853	Down	0.56693	Down	-	-
20	10.64	130.07	3-Methylene-3H-indole	C_9H_7N	-	-	0.59888	Down	-	-
21	10.89	187.06	Indoleacrylic acid	$C_{11}H_9NO_2$	-	-	-	-	2.3982	Up
22	11.65	515.29	Taurocholic acid	$C_{26}H_{45}NO_7S$	2.7502	Up	-	-	45.825	Up
23	12.22	255.13	Spermic acid	$C_{10}H_{20}N_2O_4$	-	-	-	-	1.9926	Up
24	12.50	243.18	N-Undecanoylglycine	$C_{13}H_{25}NO_3$	0.72081	Down	-	-	-	-
25	13.30	412.25	Grayanotoxin I	$C_{22}H_{36}O_7$	2.7201	Up	1.5515	Up	2.7827	Up
26	13.36	499.30	Taurodeoxycholic acid	$C_{26}H_{45}NO_6S$	-	-	-	-	26.458	Up
27	14.23	406.27	7-ketodeoxycholic acid	$C_{24}H_{38}O_5$	-	-	-	-	2.0121	Up
28	14.59	256.26	Hexadecasphinganine	$C_{16}H_{35}NO_2$	1.8545	Up	-	-	-	-
29	15.02	312.23	15,16-DiHODE	$C_{18}H_{32}O_4$	0.41898	Down	0.46882	Down	-	-
30	15.36	449.33	Spirostane-3,6-dione		-	-	53.13	Up	-	-
31	15.42	314.25	9,10-Epoxy-18-hydroxy-octadecanoic acid	$C_{18}H_{34}O_4$	-	-	0.54319	Down	-	-
32	15.80	279.23	(S)-Coriolic acid	$C_{18}H_{32}O_3$	0.41174	Down	0.47979	Down	-	-
33	15.80	314.25	12,13-DiHOME	$C_{18}H_{34}O_4$	0.48409	Down	0.48017	Down	-	-
34	16.10	467.30	PE(17:0/0:0)	$C_{22}H_{46}NO_7P$	0.54709	Down	0.75119	Down	0.79682	Down
35	16.60	372.31	Tetradecanoylcarnitine	$C_{21}H_{41}NO_4$	0.63571	Down	0.78623	Down	-	-
36	16.74	517.32	LysoPC(18:3(6Z,9Z,12Z))	$C_{26}H_{48}NO_7P$	0.49363	Down	0.70941	Down	-	-
37	16.92	477.29	LPE(18:2/0:0)	$C_{23}H_{44}NO_7P$	0.6103	Down	-	-	-	-
38	16.94	446.33	3-hydroxyarachidonoylcarnitine	$C_{27}H_{45}NO_5$	-	-	0.59265	Down	-	-
39	17.02	277.22	(6Z,9Z,12Z)-17-Hydroxy-6,9,12-octadecatrienoic acid	$C_{18}H_{30}O_3$	0.32434	Down	0.3687	Down	0.48692	Down
40	17.02	493.32	LPC(16:1(9Z)/0:0)	$C_{24}H_{48}NO_7$	0.57165	Down	0.73208	Down	0.74229	Down
41	17.23	291.20	9-J1-phytoprostane	$C_{18}H_{28}O4$	3.4158	Up	-	-	-	-
42	17.23	453.29	LysoPE(0:0/16:0)	$C_{21}H_{44}NO_7P$	0.5915	Down	-	-	-	-
43	17.43	254.22	Palmitoleic acid	$C_{16}H_{30}O_2$	-	-	0.24366	Down	-	-
44	17.49	481.32	LysoPC(15:0)	$C_{23}H_{48}NO_7P$	0.63267	Down	0.78626	Down	0.75482	Down
45	17.71	568.34	LysoPC(22:6(4Z,7Z,10Z,13Z,16Z,19Z)/0:0)	$C_{30}H_{50}NO_7P$	0.69241	Down	-	-	-	-
46	17.73	424.34	(9Z)-3-hydroxyoctadecenoylcarnitine	$C_{25}H_{47}NO_5$	0.68965	Down	-	-	-	-
47	17.95	296.24	Avenoleic acid	$C_{18}H_{32}O_3$	0.37293	Down	0.41177	Down	0.51728	Down
48	18.05	479.30	LysoPE(18:1(11Z)/0:0)	$C_{23}H_{46}NO_7P$	0.61118	Down	-	-	0.67742	Down
49	18.09	507.33	LysoPC(18:1(11Z)/0:0)	$C_{26}H_{52}NO_7P$	0.61608	Down	0.76826	Down	0.73005	Down
50	18.34	294.22	Colneleic acid	$C_{18}H_{30}O_3$	0.40602	Down	0.52639	Down	0.61186	Down
51	18.34	400.34	L-Palmitoylcarnitine	$C_{23}H_{45}NO_4$	0.66372	Down	0.79206	Down	0.71149	Down
52	18.34	569.35	LysoPC(22:5(4Z,7Z,10Z,13Z,16Z)/0:0)	$C_{30}H_{52}NO_7P$	0.57317	Down	-	-	0.65651	Down
53	18.42	249.18	(9S,10E,12Z,15Z)-9-Hydroxy-10,12,15-octadecatrienoic acid		-	-	0.61211	Down	-	-

(*Continued*)

https://doi.org/10.2147/DDDT.S514891

Table 2 (Continued).

No	Rt (min)	m/z	Metabolite	Formula	FC[a]	Trend[a]	FC[b]	Trend[b]	FC[c]	Trend[c]
54	18.48	298.25	18-hydroxyoleic acid	$C_{18}H_{34}O_3$	0.40347	Down	0.4778	Down	-	-
55	18.50	263.24	Linoleic acid	$C_{18}H_{32}O_2$	-	-	0.46331	Down	-	-
56	18.50	434.24	LysoPA(18:2(9Z,12Z)/0:0)	$C_{21}H_{39}O_7P$	-	-	0.44276	Down	-	-
57	18.56	302.23	Eicosapentaenoic acid	$C_{20}H_{30}O_2$	-	-	0.25613	Down	-	-
58	18.78	426.36	12-Hydroxy-12-octadecanoylcarnitine	$C_{25}H_{49}NO_5$	0.63837	Down	-	-	0.65434	Down
59	18.88	521.35	LysoPC(18:1(11Z))	$C_{26}H_{52}NO_7P$	0.67813	Down	-	-	-	-
60	19.14	296.24	13S-hydroxyoctadecadienoic acid	$C_{18}H_{32}O_3$	0.3632	Down	0.52419	Down	0.58977	Down
61	19.18	521.35	PC(0:0/18:1(9Z))	$C_{26}H_{52}NO_7P$	0.69932	Down	-	-	0.77301	Down
62	19.35	319.23	17,18-DiHETE	$C_{20}H_{32}O_4$	0.3668	Down	0.50734	Down	0.56997	Down
63	19.57	509.35	LysoPC(17:0/0:0)	$C_{25}H_{52}NO_7P$	0.60445	Down	0.77385	Down	0.65781	Down
64	19.59	208.18	2-Cyclotetradecen-1-one	$C_{14}H_{24}O$	-	-	0.6024	Down	-	-
65	19.65	547.36	PAF	$C_{28}H_{54}NO_7P$	0.6692	Down	0.75601	Down	0.70802	Down
66	19.75	283.26	2-Hydroxyoctadecanoic acid	$C_{18}H_{36}O_3$	-	-	0.5229	Down	-	-
67	19.97	509.35	LysoPE(20:0)	$C_{25}H_{52}NO_7P$	0.72223	Down	-	-	0.68714	Down
68	19.99	547.37	LysoPC(20:2(11Z,14Z))	$C_{28}H_{54}NO_7P$	0.68225	Down	0.77004	Down	0.6989	Down
69	20.11	276.21	Stearidonic acid	$C_{18}H_{28}O_2$	0.41922	Down	0.52006	Down	0.56736	Down
70	20.27	593.37	Povpc	$C_{29}H_{56}NO_9P$	3.5231	Up	-	-	-	-
71	20.34	252.21	Palmitolinoleic acid	$C_{16}H_{28}O_2$	-	-	0.6846	Down	-	-
72	20.46	535.37	(2R)-3-{[(2-Aminoethoxy)(hydroxy) phosphoryl]oxy}-2-hydroxypropyl (11Z)-11-docosenoate	$C_{27}H_{54}NO_7P$	0.63207	Down	-	-	-	-
73	20.91	833.60	PC(20:2(11Z,14Z)/20:4(5Z,8Z,11Z,14Z))	$C_{48}H_{84}NO_8P$	-	-	-	-	2.4332	Up
74	20.93	303.23	19-Hydroxyeicosatetraenoic acid	$C_{20}H_{32}O_3$	0.37528	Down	0.47085	Down	0.4441	Down
75	20.93	347.20	5-(2-Heptadecenyl)-1,3-benzenediol	$C_{23}H_{38}O_2$	-	-	0.43774	Down	0.48081	Down
76	21.03	278.23	Octadec-11-en-9-ynoic acid	$C_{18}H_{30}O_2$	0.56132	Down	0.65537	Down	0.71499	Down
77	21.54	219.21	11-Hexadecynal	$C_{16}H_{28}O$	0.5399	Down	0.62461	Down	-	-
78	21.60	317.25	α-Linolenic acid	$C_{21}H_{32}O_2$	-	-	0.36144	Down	-	-
79	21.74	328.24	Docosahexaenoic acid	$C_{22}H_{32}O_2$	0.51846	Down	0.40356	Down	0.62967	Down
80	21.84	330.28	MG(16:0/0:0/0:0)	$C_{19}H_{38}O_4$	-	-	1.241	Up	-	-
81	21.94	304.24	Arachidonic acid	$C_{20}H_{32}O_2$	0.67448	Down	0.79119	Down	-	-
82	22.10	572.37	LysoPC(20:1(11Z)/0:0)	$C_{28}H_{56}NO_7P$	0.68251	Down	-	-	-	-
83	22.12	245.23	2-(5,8-Tetradecadienyl) cyclobutanone	$C_{18}H_{30}O$	0.67323	Down	-	-	0.7781	Down
84	22.12	280.24	Mangiferic acid	$C_{18}H_{32}O_2$	0.68204	Down	-	-	0.78932	Down
85	22.32	330.26	Ethyl eicosapentaenoic acid	$C_{22}H_{34}O_2$	0.44517	Down	0.53647	Down	0.51019	Down
86	23.05	781.56	PC(16:0/20:4(8Z,11Z,14Z,17Z))	$C_{44}H_{80}NO_8P$	0.64692	Down	-	-	-	-
87	23.07	817.58	PS(16:1(9Z)/22:0)	$C_{44}H_{84}NO_{10}P$	0.68011	Down	-	-	-	-
88	23.09	306.26	Mead acid	$C_{20}H_{34}O_2$	-	-	0.5791	Down	0.51352	Down
89	23.29	332.27	Adrenic acid	$C_{22}H_{36}O_2$	0.52733	Down	0.60047	Down	0.57323	Down
90	23.39	282.26	(Z)-13-Octadecenoic acid	$C_{18}H_{34}O_2$	0.69156	Down	0.77427	Down	0.72151	Down
91	23.85	334.31	Anandamide	$C_{22}H_{41}NO_2$	1.8033	Up	2.3046	Up	-	-
92	24.03	385.32	O-pentadecanoylcarnitine	$C_{22}H_{43}NO_4$	-	-	1.6167	Up	-	-
93	24.03	244.19	N-Undecanoylglycine	$C_{13}H_{25}NO_3$	-	-	1.2904	Up	-	-
94	24.04	417.37	Ximenic acid	$C_{26}H_{50}O_2$	-	-	-	-	-	-
95	24.61	310.31	Stearoylethanolamide	$C_{20}H_{41}NO_2$	1.5546	Up	-	-	-	-
96	24.80	622.45	Dilauroylphosphatidylcholine	$C_{32}H_{65}NO_8P$	-	-	-	-	0.64683	Down
97	29.74	369.35	Lathosterol	$C_{27}H_{46}O$	-	-	1.4872	Up	-	-

Notes: [a]ZC vs Model; [b]ZM vs Model; [c]CBM vs Mode.

Using MetaboAnalyst, we explored the potential anti-asthma mechanisms of ZC in terms of differential metabolites. In this study, pathways ($P < 0.05$) were considered to be metabolic pathways related to the anti-asthma effects of ZC. As revealed by KEGG enrichment analysis, the model group mainly interfered with the functions of glycerophospholipid metabolism, linolenic acid metabolism, and alpha linolenic acid metabolism, resulting in asthma-related symptoms; ZM group mainly regulated four pathways: biosynthesis of unsaturated fatty acids, alpha linolenic acid metabolism, linolenic acid metabolism, and glycerophospholipid metabolism; CBM group mainly regulated pathways containing alpha-Linolenic acid metabolism, glycerophospholipid metabolism, linoleic acid metabolism and taurine and hypotaurine

metabolism; ZC group was mainly involved in the regulation of the metabolic pathway in alpha-linolenic acid metabolism, linoleic acid metabolism, biosynthesis of unsaturated fatty acids, glycerophospholipid metabolism and arachidonic acid metabolism (Figure 3D). From the quantitative analysis of the regulation of metabolic pathways, compared with that of ZM and CBM, the combined use of drugs can regulate one more.

Network Analysis

The effect of ZC on the metabolism of asthma was further explored through network pharmacology. A panel of genes that were overlapping with the genes regulated ZC and asthma targets was selected for analysis (Table S6 and Figure 4A). We screened 81 genes associated with metabolism with MetScape and identified 186 potential gene targets were with String and Cytoscape. The potential genes were calculated by Cytoscape, and 40 hub genes were screened taking the degree > 2 medians as the screening index. Additionally, a network of component-target was established (Figure 4B). Based on the Metascape website, KEGG enrichment was performed to determine the top 20 pathways (Figure 4C). The results showed that the calcium signaling pathway, Th17 cell differentiation pathway, PI3K-Akt signaling pathway, cGMP-PKG signaling pathway and arachidonic acid metabolic pathway may be the main pathway for treating asthma with these components. Then, using MetScape App of Cytoscape, we created a compound-reaction-enzyme-gene network with the hub genes using the differential metabolites from metabolomics (Figure 4D).

Association Between Plasma Metabolomics and Network Pharmacology

To explore the crucial metabolic pathways, the 62 differential metabolites and 186 targets were conducted joint pathway analysis by MetaboAnalyst. The results showed that linoleic acid metabolism, arachidonic acid metabolism, alpha-linolenic acid metabolism and glutathione metabolism were simultaneously enriched with the targets from network pharmacology and the differential metabolites from metabolomics. According to the number of targets and metabolites, arachidonic acid metabolism was selected as the most crucial metabolic pathways (Figure 5A).

Arachidonic acid can be metabolized through three pathways regulated by cyclooxygenases (COX), lipoxygenases (LOX), and cytochrome P450 (CYP450) in the body, producing numerous metabolites such as prostaglandins, thromboxanes, lipoxygens, leukotrienes, hydroxyeicosatetraenoic acid, and eicosatetraenol, which are widely involved in immune and inflammatory responses. The metabolism of arachidonic acid involved in this study was shown in Figure 5B.

Molecular Docking

The common targets of the above two parts were selected to be the core genes of anti-asthma effect induced by ZC. Finally, the five hub genes (PLA2G4A, PLA2G1B, ALOX5, CYP1A2, and CYP3A4) and five active compounds (aseperglaucide, kaempferol, diosgenin, coumaroyltyramine, isoverticine) were selected for molecular docking. Binding energy values obtained by docking with MOE are shown in Table 3. The lowest affinity between ALOX5 and asperglaucide was −7.24 kcal/mol, which is connected by one hydrogen bond; the lowest affinity between ALOX5 and kaempferol was −3.86 kcal/mol, connected by two hydrogen bonds; the lowest affinity between CYP1A2 and kaempferol was −6.96 kcal/mol, connected by three hydrogen bonds; the lowest affinity between CYP1A2 and coumaroyltyramine was −7.97 kcal/mol, connected by two hydrogen bonds; the lowest affinity between CYP3A4 and kaempferol was −6.02 kcal/mol, connected by three hydrogen bonds; the lowest affinity between CYP3A4 and diosgenin was −6.39 kcal/mol, connected by one hydrophobic bond; the lowest affinity between PLA2G4A and diosgenin was −5.79 kcal/mol, connected by two hydrogen bonds; the lowest affinity between PLA2G1B and isoverticine was −6.22 kcal/mol, connected by two hydrogen bonds. The binding modes and sites are shown in Figure 6.

Target Validation in vivo

Joint pathway analysis of targets and metabolites indicated that the arachidonic acid metabolism pathway was the most crucial metabolic pathway. Meanwhile, we validated highly relevant genes based on network pharmacology predictions and literature research. Due to the important roles in arachidonic acid metabolism, PLA2G4A, ALOX5 and CYP1A2 gene were used for further validation.[43,44] According to Figure 7, PLA2G4A, ALOX5 and CYP1A2 gene expression were significantly higher in the model group rats' lung compared with the control group ($P < 0.05$), while the expression

https://doi.org/10.2147/DDDT.S514891

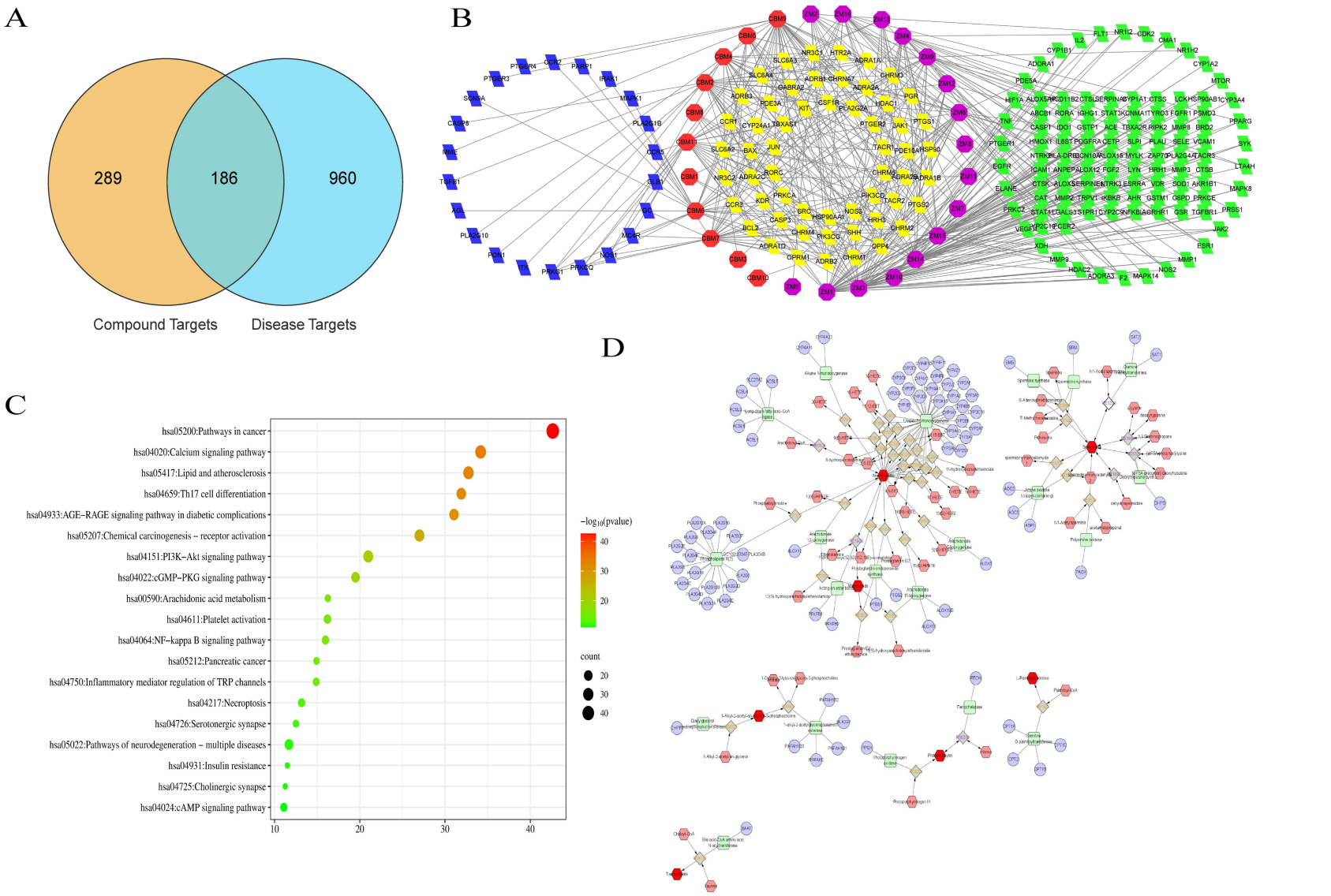

Figure 4 Network Pharmacology uncovers the mechanism of ZC for asthma. (**A**) The Venn diagram between constituents-related targets and asthma-related targets, (**B**) The network of constituents and asthma-related targets, (**C**) KEGG pathway analyses of the hub gene, (**D**) Compound-reaction-enzyme-gene networks for key metabolites and genes. The size and color are correlated to the degrees of targets in network: large size and deep color with purple means this target with high degree.

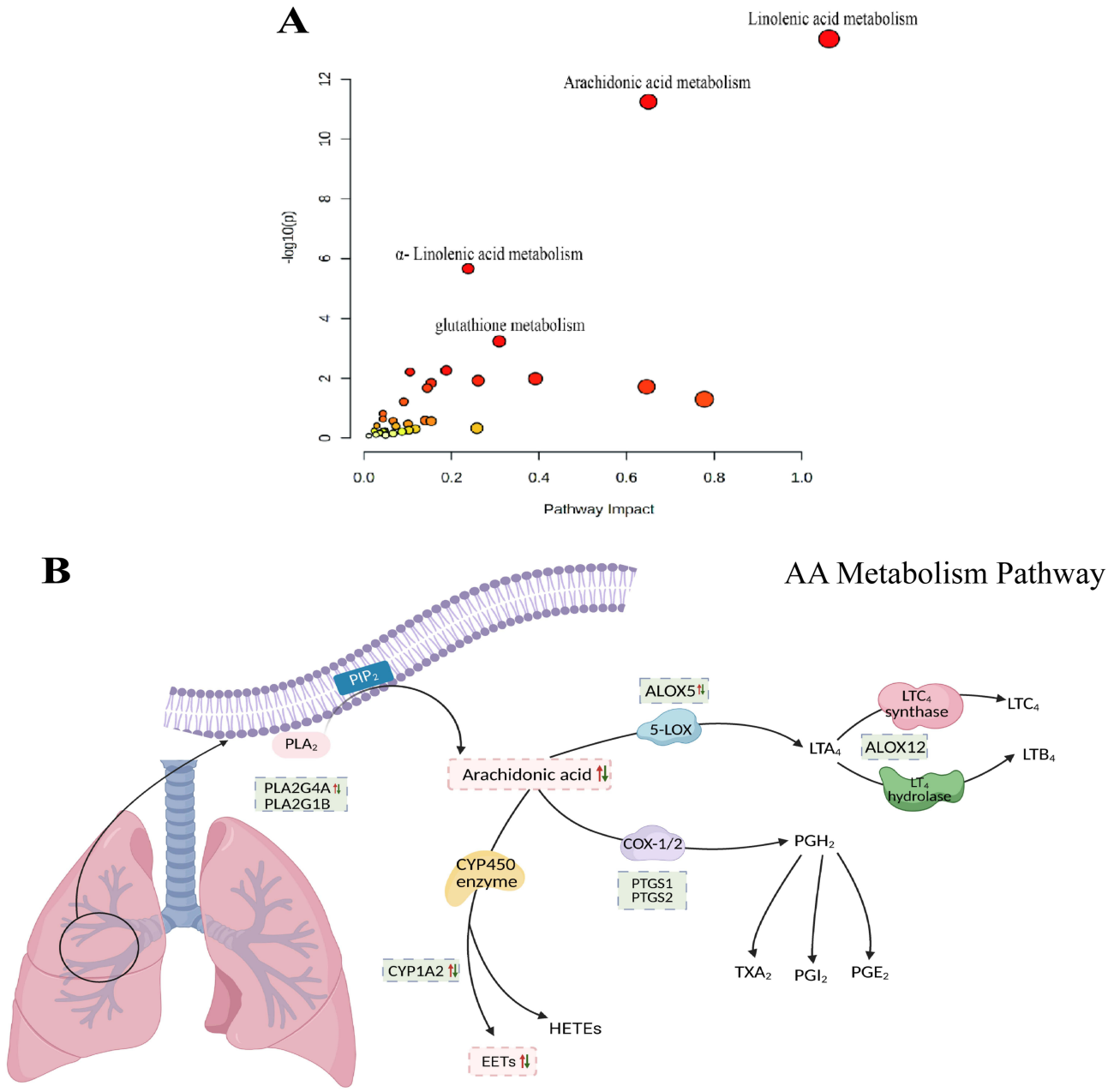

Figure 5 (**A**) Analysis of the joint pathways between metabolomics and network pharmacology; (**B**) Arachidonic acid metabolism pathway.

of PLA2G4A, ALOX5 and CYP1A2 genes in the lungs of ZC group rats was markedly reduced compared to the model group ($P < 0.05$).

Discussion

This study evaluated the anti-asthma effect of ZC by establishing an OVA-induced rat asthma model. The results showed that ZC treatment significantly improved lung function (reducing Rrs and increasing Cydn) and reduced the secretion of inflammatory factors IL-4 and IL-13. Further histological analysis confirmed that ZC alleviated lung inflammation and pathological damage. In addition, the efficacy of ZC is significantly better than monotherapy (ZM and CBM), indicating its synergistic anti-asthma effect. Asthma is a chronic airway inflammatory disease closely related to excessive activation of Th2 cells and Th1/Th2 immune imbalance.[45] The secretion of IL-4 and IL-13 by Th2 cells promotes IgE mediated

https://doi.org/10.2147/DDDT.S514891

Table 3 The Values of Lowest Affinity Between Protein and Small Molecule

Protein–Small Molecule	Affinity (kcal/mol)				
	1	2	3	Average	SD
ALOX5-asperglaucide	−7.2335	−7.1893	−7.3004	−7.2411	0.0559
ALOX5-kaempferol	−3.8852	−3.9201	−3.7745	−3.8599	0.0760
CYP1A2-kaempferol	−6.9667	−6.9012	−7.0067	−6.9582	0.0532
CYP1A2-coumaroyltyramine	−7.9699	−8.1346	−7.8178	−7.9741	0.1584
CYP3A4-kaempferol	−5.9843	−6.1357	−5.9327	−6.0176	0.1055
CYP3A4-diosgenin	−6.3344	−6.4802	−6.3568	−6.3905	0.0785
PLA2G4A-diosgenin	−5.7450	−5.9401	−5.7026	−5.7959	0.1267
PLA2G1B-isoverticine	−6.2867	−6.0128	−6.3683	−6.2226	0.1862

immune response and eosinophil infiltration, leading to airway inflammation and excessive mucus secretion.[46,47] ZC effectively alleviated these pathological changes by inhibiting the secretion of Th2 cytokines.

Our results showed that ZC could regulate 62 metabolites and five pathways, containing linoleic acid metabolism, alpha-linolenic acid metabolism, arachidonic acid metabolism and glutathione metabolism in asthma rat. Both the number of differential metabolites and metabolic pathways regulated by ZC were higher than that of monotherapy, indicating the synergistic anti-asthma effect of combination therapy. The joint metabolic pathways obtained through the metabolomics and network pharmacology were mainly enriched in linoleic acid metabolism, arachidonic acid metabolism, alpha-linolenic acid metabolism. Based on the compound-reaction-enzyme-gene network and PPI interaction network, we found that ZC affects the arachidonic acid metabolism pathway by regulating the expression of key enzyme genes such as PLA2G4A, ALOX5, and CYP1A2. These genes play a central role in the synthesis and release of inflammatory mediators.

Arachidonic acid is esterified in the form of phospholipids in the cell membrane. Phospholipase A2 (PLA2) triggers the release of arachidonic acid from cellular membranes. By blocking PLA2, inflammation can be reduced, and research on PLA2 inhibitors is becoming increasingly important in the pharmaceutical industry.[48] PLA2G4A is primarily a calcium-dependent phospholipase and lysophospholipase that participates in membrane lipid remodeling and lipid mediator synthesis during inflammatory response. It has the ability to specifically break down the sn-2 arachidonoyl group from phospholipids in cell membranes, a precursor to eicosanoid synthesis through cyclooxygenase pathway. It may also release free bioactive eicosanoids by hydrolyzing the sn-2 fatty chain of eicosanoid lysophospholipids in an alternative pathway of eicosanoid biosynthesis.[43] Arachidonic acid is mainly metabolized in *vivo* through three pathways: the cyclooxygenase pathway; lipoxygenase pathway; cytochrome P450 enzyme pathway. ALOX5 gene is involved in encoding 5-lipoxygenase and is an enzyme playing a rate limiting role in the biosynthesis pathway of leukotriene A4.[44,49] Leukotriene A4 can be converted to leukotriene B4 through leukotriene A4 hydrolase catalysis or to LTC4 through LTC4 synthase. Leukotriene B4 is an effective catalyst for neutrophils, monocytes, and eosinophils, while LTC4 and its derivative leukotriene D4 are powerful bronchoconstrictors that increase vascular permeability and trigger respiratory mucus secretion.[50,51] When the asthma response occurs, the products of 5-lipoxygenase were synthesized and released in the airway, mediating bronchial contraction and the release of inflammatory factors, playing an important role in the pathophysiology of asthma. The CYP enzyme family plays a crucial part in the metabolism of arachidonic acid. Among these, CYP1A2, CYP2C, and CYP2J2 are key epoxygenase enzymes that convert arachidonic acid into epoxyeicosatrienoic acids. Epoxyeicosatrienoic acids are known for their diverse beneficial actions, including vasodilation, anti-inflammatory properties, prevention of apoptosis, anti-thrombotic effects, natriuresis, and protection of the cardiovascular system.[52] In this study, the mRNA level of PLA2G4A, ALOX5 and CYP1A2 were significantly decreased in lung tissue in ZC groups, indicating that ZC might play a role in arachidonic acid metabolism regulation by synergetic inhibiting the activity of PLA2G4A, ALOX5 and CYP1A2.

In addition, we constructed a herb-component-target network in order to target the hub enzyme genes of the above metabolic pathways activated by ZC and found that the small molecular compounds from ZC interacting with them

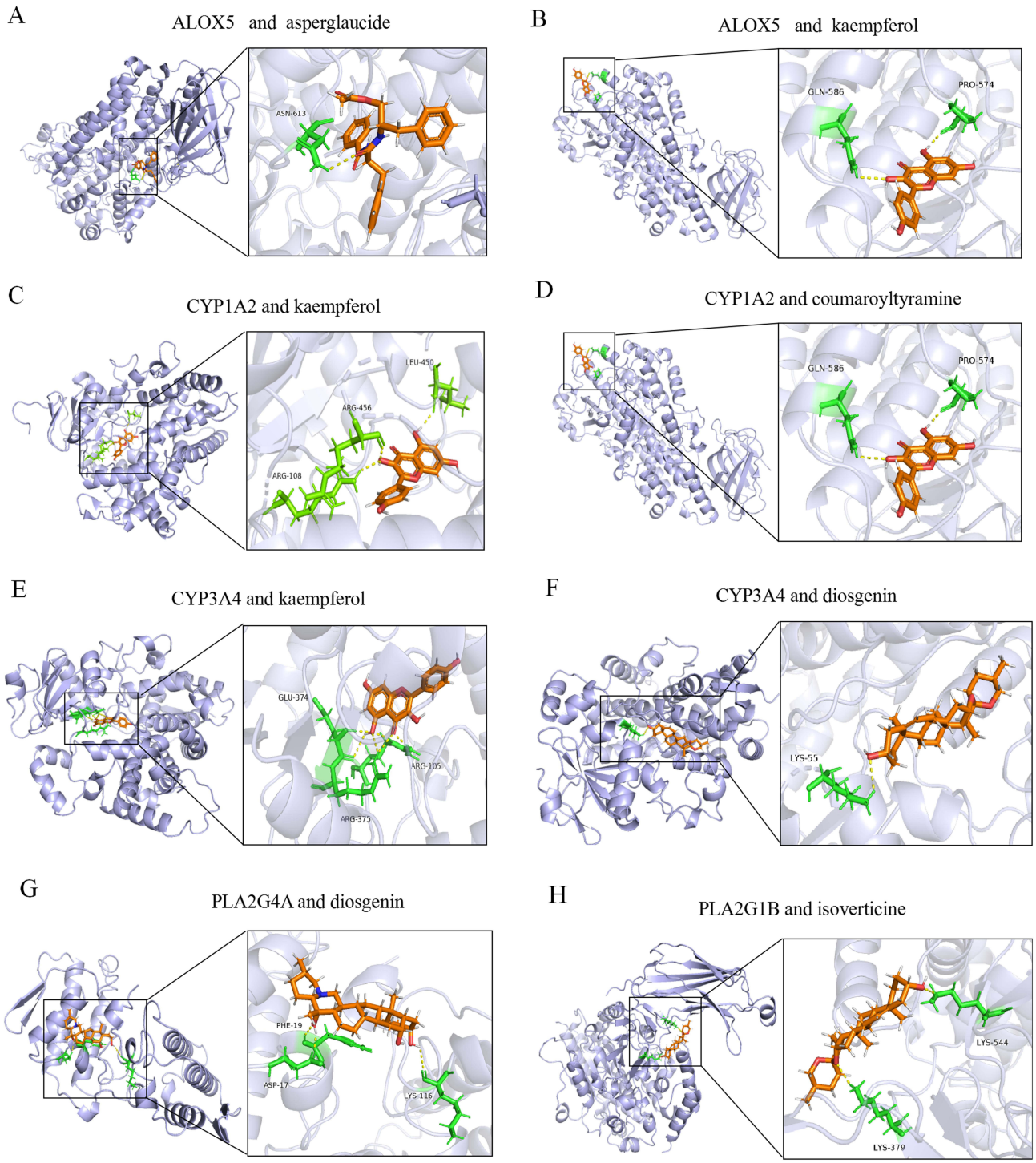

Figure 6 Docking patterns between different components and targets. (**A**) ALOX5 and asperglaucide, (**B**) ALOX5 and kaempferol, (**C**) CYP1A2 and kaempferol, (**D**) CYP1A2 and coumaroyltyramine, (**E**) CYP3A4 and kaempferol, (**F**) CYP3A4 and diosgenin, (**G**) PLA2G4A and diosgenin, (**H**) PLA2G1B and isoverticine.

included asperglaucide, kaempferol, diosgenin, coumaroyltyramine and isoveticine. Previous study showed that kaempferol inhibited airway epithelial-to-mesenchymal transition and fibrosis of endotoxin-induced epithelial cells in OVA-sensitized mice, targeting asthmatic airway constriction.[53] Additionally, this compound inhibited airway inflammation by interfering with tyrosine kinase/signal transducers and activators of transcription signaling in asthmatic mice and airway epithelial cells.[54] Diosgenin is a naturally occurring saponin compound. Traditional Chinese medicine has confirmed that

https://doi.org/10.2147/DDDT.S514891

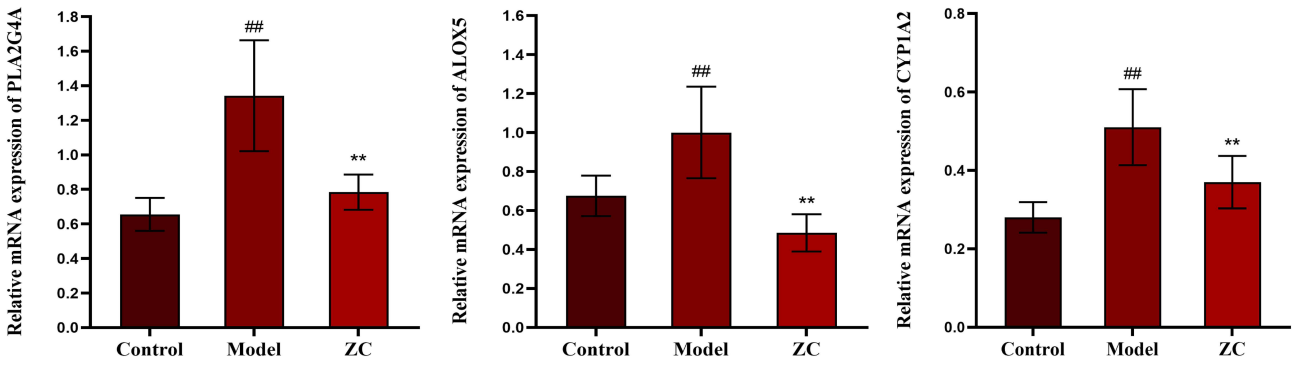

Figure 7 Relative expression of PLA2AG4, ALOX5, CYP1A2 (n = 6). ($^{\#\#}P < 0.05$ vs Control, $^{**}P < 0.05$ vs Model).

diosgenin has an expectorant effect, and modern pharmacological studies have proved that diosgenin also has desensitization, anti-inflammatory, and other effects.[55,56] Diosgenin could alleviate airway inflammation in allergic asthma mice, and its anti-inflammatory effect might be mediated by regulating the expression level of GRα, GRβ and HSP90 in airway epithelial cells.[57] It was found that imperiline and isoverticine reduced cough frequency in a dose-dependent manner. Both alkaloids showed significant anti-inflammatory effects in anti-inflammatory tests. Inflammatory diseases of the respiratory tract are often responsible for coughing, and alkaloids have anti-inflammatory properties that may help in treating coughing.[15] These results may provide a basis for developing new medications for the treatment of asthma, including complementary and alternative forms of treatment.

In summary, our study integrated drug pair extraction component identification, non targeted metabolomics, network pharmacology, molecular docking, and fluorescence quantitative PCR techniques to elucidate the molecular mechanism of Zhimu Chuanbei mother drug in the treatment of asthma. This study clarified the key role of arachidonic acid, but only validated the expression levels of individual genes, lacking overall and protein level research. In addition, the validation of active ingredients was limited to molecular docking, and further experimental validation should be needed to clarify the pharmacological substance basis for treating asthma.

Conclusion

This study utilized an integrated analysis platform including metabolomics, network pharmacology, effects evaluation, molecular docking, and RT-qPCR was established for exploration of ZC's potential molecular mechanisms in asthma treatment. It was found that ZC could regulate arachidonic acid metabolism by inhibiting PLA2G4A, ALOX5 and CYP1A2 activity in synergistic way. Those findings would provide an insight into the combination mechanisms of ZC herb pairs for anti-asthma and also clarify the TCM composition rules.

Abbreviations

ZC, Zhimu-Chuanbeimu; ZM, Zhimu; CBM, Chuanbeimu; UPLC-QTOF-MS, Ultra-high performance liquid chromatography combined with quadrupole time-of-flight mass spectrometry; TCM, Traditional Chinese Medicine; OVA, Ovalbumin; Rrs, Expiratory resistance; Cydn, Lung dynamic compliance; IL-4, Interleukin-4; IL-13, Interleukin-13; QC, Quality control; H&E, Hematoxylin and eosin; MS, Mass Spectrometry; IDA, Information-dependent acquisition; PCA, Principle component analysis; OPLS-DA, Orthogonal partial least squares-discriminant analysis; VIP, Variable Importance in Projection; FC, fold change; PLA2, Phospholipase A2.

Data Sharing Statement

The authors confirm that the data supporting the findings of this study are available within the article and its Supplementary material. Raw data that support the findings of this study are available from the corresponding author, upon reasonable request.

Ethics Approval and Consent to Participate

All animal studies were conducted according to the Guide for Care and Use of Laboratory Animals approved by the Hebei Medical University Ethics Committee (IACUC-Hebmu-2022134, Approval Date: March 28, 2022).

Acknowledgments

This work was supported by the Natural Science Foundation of Hebei Province of China (H2022206384). Talents construction project of science and technology innovation, Hebei Academy of Agriculture and Forestry Sciences (C24R0806).

Author Contributions

All authors made a significant contribution to the work reported, whether that is in the conception, study design, execution, acquisition of data, analysis and interpretation, or in all these areas; took part in drafting, revising or critically reviewing the article; gave final approval of the version to be published; have agreed on the journal to which the article has been submitted; and agree to be accountable for all aspects of the work.

Disclosure

The authors declare no competing interests.

References

1. Alberto P, Christopher B, Søren EP, Helen KR. Asthma. *Lancet*. 2018;391(10122):783–800. doi:10.1016/S0140-6736(17)33311-1
2. Ioana A, Ibon EG, Catalina C, et al. Advances and highlights in asthma in 2021. *Allergy*. 2021;00:1–18.
3. Lommatzsch M, Virchow JC. Severe asthma: definition, diagnosis and treatment. *Dtsch Arztebl Int*. 2014;111(50):847–855. doi:10.3238/arztebl.2014.0847
4. Thomas LJ, Daniel MN, Anoop JC. Diagnosis and treatment of severe asthma: a phenotype-based approach. *Clin Med*. 2018;18(2):s36–s40. doi:10.7861/clinmedicine.18-2-s36
5. Akdis CA. Therapies for allergic inflammation: refining strategies to induce tolerance. *Nat Med*. 2012;18(5):736–749.
6. Byrne PO, Fabbri LM, Pavord ID, Papi A, Petruzzelli S, Lange P. Asthma progression and mortality: the role of inhaled corticosteroids. *Eur Respir J*. 2019;54(1):1900491. doi:10.1183/13993003.00491-2019
7. Li J, Zhang F, Li J. The immunoregulatory effects of traditional Chinese medicine on treatment of asthma or asthmatic inflammation. *Am J Chin Med*. 2015;43(6):1059–1081.
8. Zhang HP, Wang L, Wang Z, et al. Chinese herbal medicine formula for acute asthma: a multi-center, randomized, double-blind, proof-of-concept trial. *Respir Med*. 2018;140:42–49. doi:10.1016/j.rmed.2018.05.014
9. Qu L, Zhou Y. Effect of ermu powder on pulmonary function in elderly chronic obstructive pulmonary disease patients with pulmonary yin deficiency in stable stage. *Acta Chin Med*. 2018;33(07):1197–1202.
10. Wang JW, Wu S, Tang CY. Research on statistics and drug compatibility of cough treatment prescriptions by traditional Chinese medicine. *Jilin J Trad Chin Med*. 2014;34(4):419–420.
11. Zeng YJ, Yang Y. Summary of traditional Chinese medicine pairs commonly used in the treatment of pulmonary diseases by professor Yang Yi. *Asia-Pac Trad Med*. 2017;13(19):77–78.
12. Yeum HS, Lee YC, Kim SH, Roh SS, Lee JC, Seo YB. *Fritillaria cirrhosa Anemarrhena asphodeloides*, Lee-Mo-Tang and cyclosporine a inhibit ovalbumin-induced eosinophil accumulation and Th2-mediated bronchial hyperresponsiveness in a murine model of asthma. *Basic Clin Pharmacol Toxicol*. 2007;100(3):205–213. doi:10.1111/j.1742-7843.2007.00043.x
13. Li SZ. *Compendium of Materia Medica*. Beijing: The People's Health Press Co. Ltd; 1975.
14. Liu YP. Progress on pharmacological activities and mechanism of Anemarrhena saponin. *J Pharm Pract*. 2018;36(01):24–29.
15. Wang DD, Wang S, Chen X, et al. Antitussive, expectorant and anti-inflammatory activities of four alkaloids isolated from bulbus of *Fritillaria wabuensis*. *J Ethnopharmacol*. 2012;139(1):189–193. doi:10.1016/j.jep.2011.10.036
16. Zhang X, Zheng X. Exploring traditional Chinese medicine treatment of bronchial asthma from the perspective of Yingwei Qi and blood theory. *Hubei J Trad Chin Med*. 2016;38(9):53–54.
17. Tian X, Hou JL, Yang MX, et al. Characterization of Fritillariae cirrhosae bulbus from multiple sources by potential Q-marker based on metabolomics and network pharmacology. *Rapid Commun Mass Spectrom*. 2023;37(1):e9403. doi:10.1002/rcm.9403
18. Sun YG, Du YF, Yang K, et al. A comparative study on the pharmacokinetics of a traditional Chinese herbal preparation with the single herb extracts in rats by LC-MS/MS method. *J Pharm Biomed Anal*. 2013;81: 34–43.
19. Johnson CH, Ivanisevic J, Siuzdak G. Metabolomics: beyond biomarkers and towards mechanisms. *Nat Rev Mol Cell Biol*. 2016;17(7):451–459. doi:10.1038/nrm.2016.25
20. Yuan H, Ma Q, Cui H, et al. How can synergism of traditional medicines benefit from network pharmacology?. *Molecules*. 2017;22(7):1135. doi:10.3390/molecules22071135
21. Yang M, Lao L. Emerging applications of metabolomics in traditional Chinese medicine treating hypertension: biomarkers, pathways and more. *Front Pharmacol*. 2019;10:158. doi:10.3389/fphar.2019.00158

22. Luo TT, Lu Y, Yan SK, Xiao X, Rong XL, Guo J. Network pharmacology in research of Chinese medicine formula: methodology, application and prospective. *Chin J Integr Med*. 2020;26(1):72–80. doi:10.1007/s11655-019-3064-0
23. Wang N, Zhu F, Shen M, et al. Network pharmacology-based analysis on bioactive anti-diabetic compounds in Potentilla discolor Bunge. *J Ethnopharmacol*. 2019;241:111905. doi:10.1016/j.jep.2019.111905
24. Huang J, Cheung F, Tan HY, et al. Identification of the active compounds and significant pathways of yinchenhao decoction based on network pharmacology. *Mol Med Rep*. 2017;16(4):4583–4592. doi:10.3892/mmr.2017.7149
25. Julio C. The latest automated docking technologies for novel drug discovery. *Expert Opin Drug Discov*. 2020;16(6):625–645.
26. Li X, Wei SZ, Niu SQ, et al. Network pharmacology prediction and molecular docking-based strategy to explore the potential mechanism of Huanglian Jiedu decoction against sepsis. *Comput Biol Med*. 2022;144:105389. doi:10.1016/j.compbiomed.2022.105389
27. Ru J, Li P, Wang J, et al. TCMSP: a database of systems pharmacology for drug discovery from herbal medicines. *J Cheminf*. 2014;6(1):13. doi:10.1186/1758-2946-6-13
28. Tian X, Wei JH, Niu YK, et al. Investigation of pharmacodynamic material basis of Anemarrhenae Rhizoma and its processed products based on plant metabolomics and molecular docking technology. *Rapid Commun Mass Spectrom*. 2023;37(7):e9473. doi:10.1002/rcm.9473
29. Ye H, Ye L, Kang H, et al. HIT: linking herbal active ingredients to targets. *Nucleic Acids Res*. 2011;39(Database issue):D1055–D1059. doi:10.1093/nar/gkq1165
30. Daina A, Michielin O, Zoete V. SwissTargetPrediction: updated data and new features for efficient prediction of protein targets of small molecules. *Nucleic Acids Res*. 2019;47(W1):W357–W364. doi:10.1093/nar/gkz382
31. Rappaport N, Fishilevich S, Nudel R, et al. Rational confederation of genes and diseases: NGS interpretation via GeneCards, MalaCards and VarElect. *Biomed. Eng. Online*. 2017;16(Suppl. 1):72. doi:10.1186/s12938-017-0359-2
32. Amberger JS, Hamosh A. Searching Online Mendelian Inheritance in Man (OMIM): a knowledgebase of human genes and genetic phenotypes. *Curr Protoc Bioinformatics*. 2017;58(1):1.2.1–1.2.12. doi:10.1002/cpbi.27
33. Wang Y, Zhang S, Li F, et al. Therapeutic target database 2020: enriched resource for facilitating research and early development of targeted therapeutics. *Nucleic Acids Res*. 2020;48(D1):D1031–D1041. doi:10.1093/nar/gkz981
34. Wishart DS, Feunang YD, Guo AC, et al. DrugBank 5.0: a major update to the drugbank database for 2018. *Nucleic Acids Res*. 2018;46(D1): D1074–D1082. doi:10.1093/nar/gkx1037
35. Szklarczyk D, Gable A, Lyon D, et al. STRING v11: protein–protein association networks with increased coverage, supporting functional discovery in genome-wide experimental datasets. *Nucleic Acids Res*. 2019;47(D1):D607–D613. doi:10.1093/nar/gky1131
36. Shannon P, Markiel A, Ozier O, et al. Cytoscape: a software environment for integrated models of biomolecular interaction networks. *Genome Res*. 2003;13(11):2498–2504. doi:10.1101/gr.1239303
37. Zhou YY, Zhou B, Lars P, et al. Metascape provides a biologist-oriented resource for the analysis of systems-level datasets. *Nat Commun*. 2019;10 (1):1523. doi:10.1038/s41467-019-09234-6
38. Zhang WD, Chen Y, Jiang H, et al. Integrated strategy for accurately screening biomarkers based on metabolomics coupled with network pharmacology. *Talanta*. 2020;211:120710. doi:10.1016/j.talanta.2020.120710
39. Gross C, Seroogy KB. Chapter 6 - neuroprotective roles of neurotrophic factors in depression. In: Gozes I, Levine J, editors. *Neuroprotection in Autism, Schizophrenia and Alzheimer's Disease*. Academic Press; 2020:125–144.
40. Li JX, Li RZ, Sun A, et al. Metabolomics and integrated network pharmacology analysis reveal Tricin as the active anti-cancer component of Weijing decoction by suppression of PRKCA and sphingolipid signaling. *Pharmacol Res*. 2021;171:105574. doi:10.1016/j.phrs.2021.105574
41. Yuan Y, He Y, Wasti B, et al. lncRNA CRNDE affects Th17/IL-17A and inhibits epithelial-mesenchymal transition in lung epithelial cells reducing asthma signs. *Oxid Med Cell Longev*. 2023;2023:2092184. doi:10.1155/2023/2092184
42. Tang WF, Dong M, Teng FZ, et al. Environmental allergens house dust mite-induced asthma is associated with ferroptosis in the lungs. *Exp Ther Med*. 2021;22(6):1–10. doi:10.3892/etm.2021.10918
43. Plastira I, Bernhart E, Joshi L, et al. MAPK signaling determines lysophosphatidic acid (LPA)-induced inflammation in microglia. *J Neuroinflammation*. 2020;17(1):127–143. doi:10.1186/s12974-020-01809-1
44. Sinham S, Doble M, Manju SL. 5-lipoxygenase as a drug target: a review on trends in inhibitors structural design, SAR and mechanism based approach. *Bioorg Med Chem*. 2019;27(17):3745–3759. doi:10.1016/j.bmc.2019.06.040
45. Lin H, Chen WF. Effects of all - trans retinoic acid on Th1 / Th2 balance in asthmatic rat models. *Biotechnology*. 2024;34(1):91–95.
46. Lee SY, Bae CS, Seo NS, et al. Camellia japonica oil suppressed asthma occurrence via GATA-3 & IL-4 pathway and its effective and major component is oleic acid. *Phytomedicine*. 2019;57:84–94. doi:10.1016/j.phymed.2018.12.004
47. Kasaian MT, Donaldson DD, Tchistiakova L, et al. Efficacy of IL-13 neutralization in a sheep model of experimental asthma. *Am J Respir Cell Mol Biol*. 2007;36(3):368–376. doi:10.1165/rcmb.2006-0244OC
48. Miyaura C, Inada M, Matsumoto C, et al. An essential role of cytosolic phospholipase A2alpha in prostaglandin E2-mediated bone resorption associated with inflammation. *J Exp Med*. 2003;197(10):1303–1310. doi:10.1084/jem.20030015
49. Sun QY, Zhou HH, Mao XY. Emerging roles of 5-lipoxygenase phosphorylation in inflammation and cell death. *Oxid Med Cell Longev*. 2019;2019 (1):2749173.
50. Bruno F, Spaziano G, Liparulo A, et al. Recent advances in the search for novel 5-lipoxygenase inhibitors for the treatment of asthma. *Eur J Med Chem*. 2018;153:65–72. doi:10.1016/j.ejmech.2017.10.020
51. Schexnaydre EE, Gerstmeier J, Garscha U, Jordan PM, Werz O, Newcomer ME. A 5-lipoxygenase-specific sequence motif impedes enzyme activity and confers dependence on a partner protein. *Biochim Biophys Acta Mol Cell Biol Lipids*. 1864;4:543–551.
52. Zordoky BNM, EI-Kadi AOS. Effect of cytochrome P450 polymorphism on arachidonic acid metabolism and their impact on cardiovascular diseases. *Pharmacol Ther*. 2010;125(3):446–463.
53. Gong JH, Cho IH, Shin D, Han SY, Park SH, Kang YH. Inhibition of airway epithelial-to-mesenchymal transition and fibrosis by kaempferol in endotoxin-induced epithelial cells and ovalbumin-sensitized mice. *Lab Investig*. 2014;94(3):297–308. doi:10.1038/labinvest.2013.137
54. Gong JH, Shin D, Han SY, et al. Blockade of airway inflammation by kaempferol via disturbing Tyk-STAT signaling in airway epithelial cells and in asthmatic mice. *Evid Based Complement Altern Med*. 2013;2013(1):250725.
55. Liang X, Wang J, Chen W, et al. Inhibition of airway remodeling and inflammation by isoforskolin in PDGF-induced rat ASMCs and OVA-induced rat asthma model. *Biomed Pharmacother*. 2017;95(5):275–286.

56. Zhu B, Dong J, Gao X, He YF, Sun HX. Antiasthmatic effects of sanglong pingchuan decoction through inducing a balanced Th1/Th2 immune response. *Evid Based Complement Alternat Med*. 2018;12(5):262–265.
57. Li XQ, Wu N, Yu RH, Guan C, Xu T, Wu JX. Effect of dioscin on glucocorticoid receptor of airway epithelial cells in mice with asthma. *Shandong Med J*. 2017;57(42):16–19.

Drug Design, Development and Therapy

Dovepress
Taylor & Francis Group

Publish your work in this journal

Drug Design, Development and Therapy is an international, peer-reviewed open-access journal that spans the spectrum of drug design and development through to clinical applications. Clinical outcomes, patient safety, and programs for the development and effective, safe, and sustained use of medicines are a feature of the journal, which has also been accepted for indexing on PubMed Central. The manuscript management system is completely online and includes a very quick and fair peer-review system, which is all easy to use. Visit http://www.dovepress.com/testimonials.php to read real quotes from published authors.

Submit your manuscript here: https://www.dovepress.com/drug-design-development-and-therapy-journal